Catalysis Letters 24 (1994) 303–315

Surface properties of iron–titania photocatalysts employed for 4-nitrophenol photodegradation in aqueous TiO_2 dispersion

L. Palmisano [1], M. Schiavello, A. Sclafani

Dipartimento di Ingegneria Chimica dei Processi e dei Materiali, Università di Palermo, Viale delle Scienze, 90128 Palermo, Italy

C. Martin, I. Martin and V. Rives

Departamento de Química Inorgánica, Universidad de Salamanca, Facultad de Farmacia, 37007 Salamanca, Spain

Received 13 September 1993; accepted 16 November 1993

Iron(III) doped specimens (0.01–5% atomic Fe : Ti) have been prepared by impregnating polycrystalline "home prepared" TiO_2 (mainly anatase) and have been studied for photocatalytic degradation of 4-nitrophenol in aqueous dispersions. Some structural and surface properties have been studied by X-ray diffraction, specific surface area and porosity measurements and FTIR monitoring of pyridine, ammonia and methanoic acid adsorption for surface acidity and basicity. Their surface properties were compared with a corresponding series of photocatalysts prepared by a coprecipitation method. Adsorption of pyridine and ammonia indicates the presence of surface acid Lewis sites, a low concentration of surface Brønsted sites being present only in the samples prepared by impregnation. The photocatalytic experiments indicated that the presence of iron ions does not influence or is detrimental for the occurrence of the 4-nitrophenol photodegradation.

Keywords: 4-nitrophenol photodegradation; iron–titania FTIR study; Brønsted and Lewis surface acid sites

1. Introduction

Iron doped polycrystalline titania powders have been extensively studied in the last years as they have drawn interest both for their surface and structural properties [1–5] and for their photoactivity in catalytic processes [6–11].

Both the bulk and surface physico-chemical properties and the photoactivity strongly depend on the methods used for the preparation of the specimens: in parti-

[1] To whom correspondence should be addressed.

cular the temperature to which the specimens are heated, the concentration of the dopant and the presence of impurities in the lattice and/or on the surface [1,2,10,11].

Although a direct correlation between surface properties and the photoactivity of the specimens is not always possible, to test doped titania specimens prepared by different methods in photodegradation reactions carried out in aqueous medium is of great importance in photocatalysis. The thorough characterization of the specimens by various techniques, moreover, could be useful to obtain a better understanding of this complex system.

In the present work the FTIR technique, using as probe molecules pyridine, ammonia and methanoic acid, was used to assess the surface acidity and basicity of a series of iron doped titania specimens obtained by impregnating pure "home prepared" TiO_2 (mainly anatase) with an aqueous solution containing Fe(III) ions.

Some coprecipitated specimens [2,10,11], were also prepared and investigated for comparison.

X-ray diffraction, specific surface areas and pore size distribution measurements were carried out of all of the specimens.

Moreover, the impregnated specimens were tested for the photodegradation of 4-nitrophenol in aqueous dispersions and their photoreactivity is discussed.

2. Experimental

2.1. CATALYST PREPARATION

Two series of solids were prepared. One series of samples was obtained by impregnating a "home prepared" TiO_2 (mainly anatase), thereafter indicated as TiO_2 "hp". The samples had nominal concentration of 0.01; 0.02; 0.04; 0.1; 0.5; 1.0; 3.0; 5.0 mol of iron per 100 mol of titanium. The preparation was carried out as follows: titanium hydroxide was precipitated by reacting an aqueous solution of $TiCl_3$ (15% Carlo Erba) with an aqueous solution of ammonia (25%, Merck), which was added dropwise at room temperature with vigorous stirring owing to the exothermicity of the reaction. The solid was filtered and washed repeatedly to remove residual Cl^- ions (tested as $AgCl_{(s)}$). Subsequently it was dried at 393 K for 24 h and finally fired in air for 24 h at 823 K. The obtained solid was divided in different fractions and each of them was impregnated with an aqueous solution containing the required amount of Fe^{3+} ions (e.g. $Fe(NO_3)_3 \cdot 9H_2O$, Merck). After standing for 24 h at room temperature, the solids were dried at 24 h at 393 K and finally fired in air for 24 h at 823 K.

The second series of solids was prepared by co-precipitation of iron and titanium hydroxides with ammonia in a similar way as that above described for the TiO_2 "hp" and subsequently by drying and heating the specimens with the same procedure and at the same temperatures as those reported above for the impreg-

nated specimens. The samples had nominal concentration of 0.02; 0.2; 0.5; and 1.0 mol of iron per 100 mol of titanium. Details of the preparation method are reported in literature [2,11].

The code used in the following for designating the samples is TFXY (X = atomic Fe percentage; Y = I or C, depending on preparation via impregnation or co-precipitation).

2.2. X-RAY DIFFRACTION

X-ray diffraction patterns were recorded on a Siemens-55 diffractometer with Ni-filtered Cu Kα1 radiation (λ = 154.05 pm) and interfaced to a DACO-MP data acquisition microprocessor provided with Diffract/AT software.

2.3. SURFACE AREA DETERMINATION AND POROSITY

Specific surface areas (BET) of all of the catalysts were determined by N_2 adsorption at 77 K, using the single-point method [12] in a Micromeritics Flowsorb II-2300 apparatus. Porosity was monitored from the adsorption–desorption isotherms at 77 K of nitrogen (from Sociedad Española del Oxigeno, SEO, Spain), measured in a conventional high vacuum system (residual pressure ca. 10^{-4} N m^{-2}), provided with a McLeod gauge, silicon oil diffusion pump and MKS Baratron pressure transducer.

2.4. INFRARED SPECTROSCOPY

The Fourier-transform infrared spectra were recorded in a 16-PC Perkin Elmer spectrometer (nominal resolution 2 cm^{-1}, averaging 100 scans). A special pyrex cell that allows recording of the spectra in vacuum or under a controlled atmosphere was used. The procedure was performed as follows: The solid was calcined at 673 K for 2 h in the cell in order to eliminate any organic impurities adsorbed during preparation. The sample was outgassed at 673 K for 2 h at a residual pressure of ca. 10^{-3} N m^{-2}, and, after cooling to room temperature, it was equilibrated with ammonia, pyridine or methanoic acid vapors, and then outgassed at increasing temperature up to 673 K. The spectrum of the solid was subtracted using the software facilities provided by the spectrometer. Only the wavenumber ranges where the significant bands due to vibrational modes of the different adsorbed species appear will be shown in the figures below.

2.5. APPARATUSES AND PROCEDURES FOR THE PHOTOREACTIVITY TESTS

A pyrex batch photoreactor of cylindrical shape containing 1.5 ℓ of aqueous dispersion was used. The photoreactor was provided with five ports in its upper section for the inlet and outlet of gases, for sampling and for pH and temperature

measurements. A 500 W medium pressure Hg lamp (Helios Italquartz, Italy) was immersed within the photoreactor and the photon flux, measured using an radiometer UVP "UVX Digital", was 16.3 mW cm^{-2}. The catalyst concentration and the 4-nitrophenol initial concentration used were 1.00 g ℓ^{-1} and 50 mg ℓ^{-1}, respectively. The initial pH of the dispersion was 4.5 and the temperature inside the reactor was about 300 K. The photoreactivity runs lasted 1 h and the samples, withdrawn every 10 min, were centrifuged to separate the solid catalyst; the 4-nitrophenol concentration in the supernatant liquid was measured by exploiting its absorption peak at 315 nm in the UV region. Further details of the apparatus and procedure can be found in literature [13,14].

3. Results and discussion

3.1. X-RAY DIFFRACTION

Samples with iron content lower than 3% (atomic), prepared both by impregnation or coprecipitation, show lines similar to that of the TiO_2 "hp" and no peak due to any other phase is recorded. The intense peaks correspond to anatase, although some minor peaks can be attributed to rutile. For iron loadings higher than 3%, weak peaks due to F_2O_3 (hematite) are also recorded. In such a case, no increase in the intensities of the rutile peaks is observed. So, it should be concluded that incorporation of iron does not catalyse the anatase → rutile phase transformation, at least at the temperature of 823 K at which the specimens were heated.

3.2. SURFACE AREA DETERMINATION AND POROSITY

Specific surface areas of the samples are reported in table 1. In all cases, values coincide (within experimental methods) when calculated following the single-

Table 1
Specific surface areas of the samples

Sample	SSA (m^2 g^{-1})	Sample	SSA (m^2 g^{-1})
TiO_2 "hp"	51	TF0.02C	53
		TF0.2C	56
TF0.01I	47	TF0.5C	68
TF0.02I	48	TF1.0C	44
TF0.04I	48		
TF0.1I	58		
TF0.5I	59		
TF1.0I	56		
TF3.0I	56		
TF5.0I	55		

point, BET, cumulative surface area [12] and *t*-plot methods [15]. For the impregnated specimens, as the iron content is increased, a small increase in the specific surface area is observed, up to the sample TF0.5I. Further increases in iron content give rise to a decrease. A similar trend is observed in samples prepared by co-precipitation, the maximum specific surface area development corresponding also to sample containing 0.5% iron.

The nitrogen adsorption/desorption curves at 77 K, fig. 1, show in all cases a type-A hysteresis loop, due to the existence of cylindrical pores open at both ends, where, according to Cohan [16] it is expected that pores of a given radius will fill at a higher P/P_0 then when they will be empty. As the iron content is increased, the hysteresis loop becomes narrower, probably owing to blocking of these pores.

Pore-size distribution curves in fig. 2 indicate a similarity among all samples studied. So, pores with a diameter close to 3.0 nm dominate in all cases, although contribution by pores with an average diameter of 4–5 nm cannot be neglected.

The *t*-plots in fig. 3 are also very similar, with upward deviations for high *t*-values. This deviation is due to condensation into large pores commencing when the slope starts to increase.

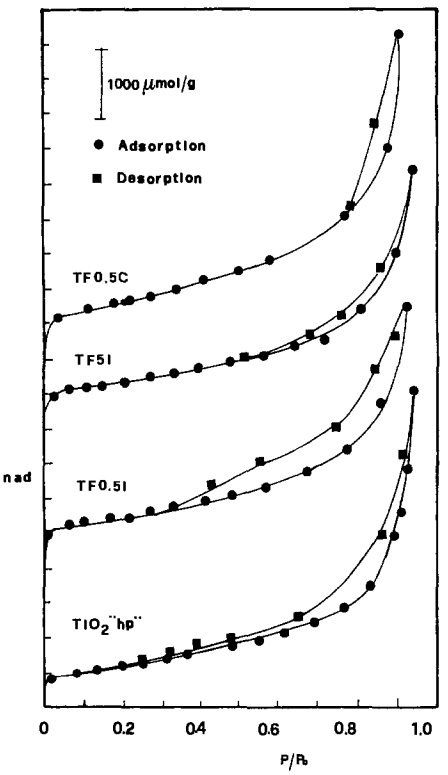

Fig. 1. Nitrogen adsorption–desorption isotherms at 77 K.

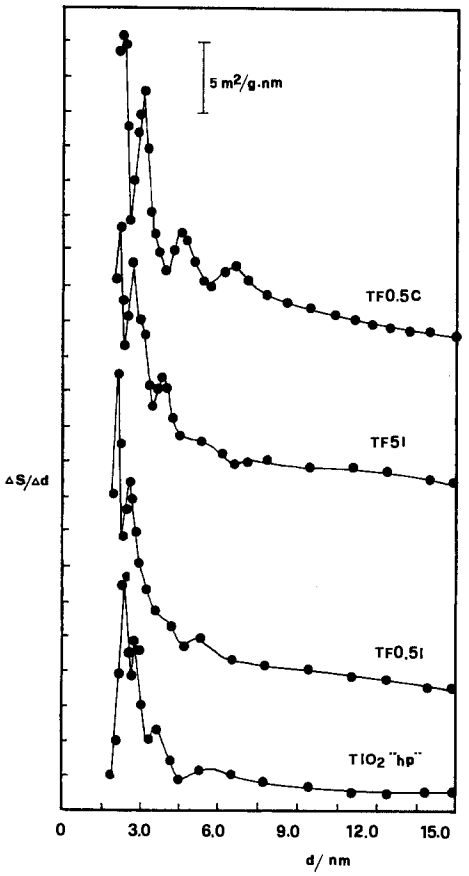

Fig. 2. Pore size distribution curves for the samples given.

3.3. INFRARED SPECTROSCOPY

Surface acidity and basicity of this system was studied by FTIR spectroscopic monitoring of the adsorption of pyridine, ammonia and methanoic acid. The use of two different probe molecules for surface acidity assessment allows selective determination of surface acid sites with different strength, due to the different basicity of both molecules [17,18].

3.3.1. Adsorption of pyridine

In figs. 4A and 4B are reported, for the sake of brevity, only the spectra recorded upon adsorption of pyridine on the samples TF0.5I and TF5I. All the doped specimens prepared both by impregnation and coprecipitation show a similar behaviour and the spectra are very similar to those recorded for pyridine adsorbed on support TiO_2 "hp" [19].

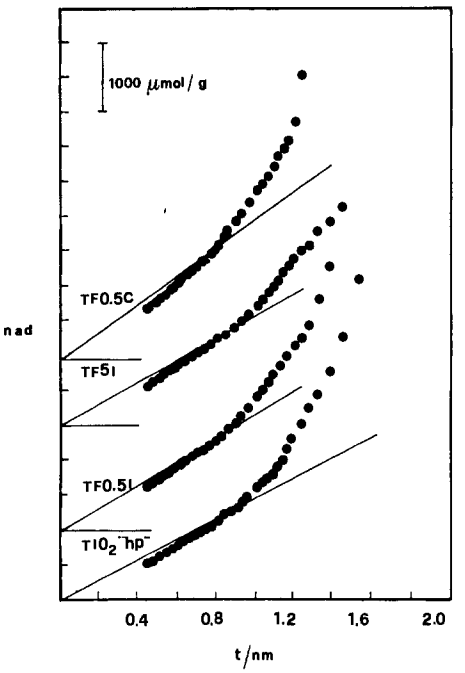

Fig. 3. t-plots for the samples given.

In the low wavenumber range, bands were recorded at 1608 ± 2, 1574, 1492 and 1443 cm^{-1}. These bands can be ascribed to stretching modes 8a, 8b, 19a and 19b of the pyridine ring, when coordinated to surface Lewis acid sites, i.e. coordinatively unsaturated species (Ti^{4+}, Fe^{3+} or Fe^{2+}). No band has been recorded that

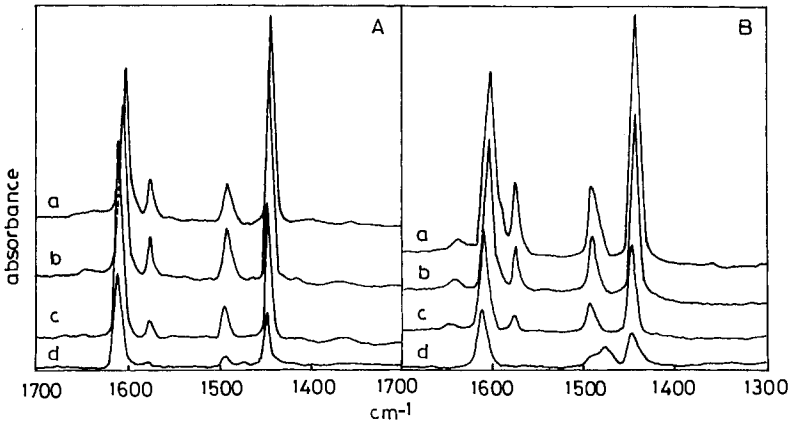

Fig. 4. FTIR spectra corresponding to adsorption of pyridine at room temperature on samples (A) TF0.5I and (B) TF5I, and outgassed at (a) room temperature, (b) 373 K, (c) 473 K, and (d) 573 K.

could be ascribed to pyridinium species, and so the presence of surface Brønsted acid sites should be discarded.

When the samples were outgassed at increasing temperatures, a general decrease of the intensities of all the bands was observed, with a simultaneous shift of the 8a and 19b bands towards larger wavenumbers. Decomposition of coordinated pyridine was observed when the samples were outgassed at 573 K, and finally all bands due to adsorbed species were removed when the samples were outgassed at 673 K.

3.3.2. Adsorption of ammonia

In figs. 5A and 5B are reported the FTIR spectra recorded upon adsorption of ammonia on the samples TF0.5I and TF0.5C, respectively. The spectra are very similar to those recorded upon adsorption of ammonia on TiO_2 "hp" [20].

For samples prepared by impregnation, two intense bands were recorded at 1603 and 1148 cm^{-1}, due to δ_{as} and δ_s modes of ammonia coordinated to surface acid Lewis sites (Fe^{3+} and Ti^{4+}). A lower intensity band was also recorded at 1360 cm^{-1}, the intensity of which decreases as the iron content is increased. This band was not recorded in the case of the samples prepared by coprecipitation (see fig. 5B). This band can be tentatively ascribed to δ(N–H) of NH_4^+ species, thus indicating the presence of surface Brønsted acid sites; their developing has been observed when other transition metal cations are incorporated into titania. It should be noted that Brønsted sites have not been detected by adsorption of pyridine, but it has been claimed that the larger basicity and the lower size of the ammonia molecule would account for such a selectivity in detection of surface acid sites.

After outgassing at increasing temperature, a decrease in the width of the bands was observed, especially those corresponding to symmetric and antisymmetric deformation modes of coordinated ammonia, and the maxima shift from 1603 to

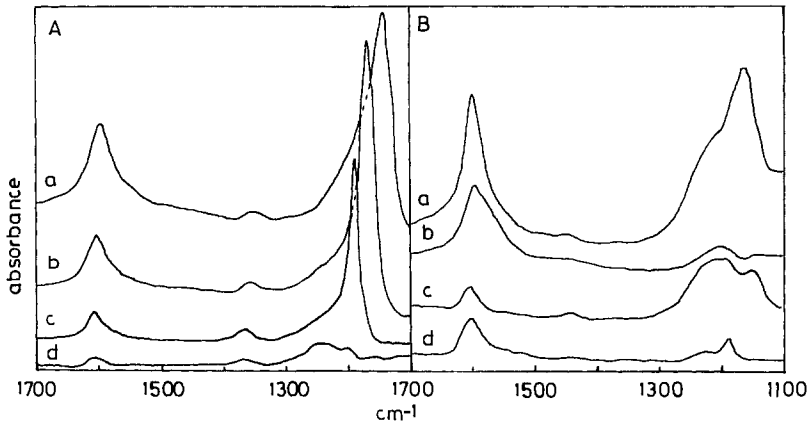

Fig. 5. FTIR spectra corresponding to adsorption of ammonia at room temperature on samples (A) TF0.5I and (B) TF0.5C, and outgassed at (a) room temperature, (b) 373 K, (c) 473 K, and (d) 573 K.

1609 cm^{-1} and from 1149 to 1200 cm^{-1}. Outgassing at 573 K removed all the bands due to adsorbed species. This shift was extremely large and, taking into account the large width of the bands recorded for the not-outgassed samples, it can be assumed that two types of Lewis acid sites exist in these samples. The outgassing removes ammonia only from those sites responsible for the low wavenumber bands (weaker surface Lewis acid sites) that according to some authors [21] correspond to adsorption on coordinatively unsaturated surface Fe^{3+} species.

The behaviour shown by the samples prepared by coprecipitation is rather similar, fig. 5B. The main difference is that the band due to δ_s mode of adsorbed ammonia is ill-defined, very broad and with different maxima between 1250 and 1150 cm^{-1}.

3.3.3. Adsorption of methanoic acid

Adsorption and outgassing of methanoic acid at room temperature leads to spectra with bands at 2956 and 2987 cm^{-1} (not shown), due to ν(C–H) stretching modes. In the low wavenumber region (fig. 6), the bands recorded at 1660 and 1288 cm^{-1} are due to molecularly adsorbed methanoic acid, while the bands at 1560, 1383 and 1353 cm^{-1} are due to ν_{as} and ν_s of carboxylate ($-COO^-$) species coordinated as a bidentate ligand [22,23], thus indicating a dissociative adsorption of methanoic acid. When the samples were outgassed at increasing temperatures, the bands became better resolved, and those due to molecularly adsorbed methanoic acid were removed. On the contrary, bands due to methanoate species remained even after outgassing at 673 K, thus indicating that these species are very stable. Nevertheless, the spectra are rather similar, thus indicating that surface basicity is very similar in all cases.

Dissociative adsorption of methanoic acid on these samples can follow two different pathways:

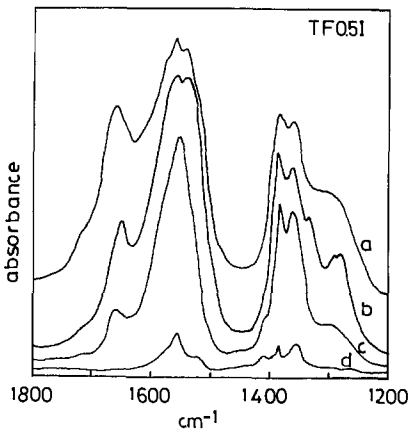

Fig. 6. FTIR spectra corresponding to adsorption of methanoic acid at room temperature on sample (A) TF0.5I and outgassed at (a) room temperature, (b) 373 K, (c) 473 K, and (d) 573 K.

$$H{-}COOH + O^{2-}_{(s)} \rightarrow H{-}COO^{-}_{(s)} + OH^{-}_{(s)}\,, \tag{1}$$

$$H{-}COOH + OH^{-}_{(s)} \rightarrow H{-}COO^{-}_{(s)} + H_2O_{(ads)}\,, \tag{2}$$

and thus, analysis of the 4000–3000 cm^{-1} range would indicate which pathway reaction occurs, as in this region the bands due to ν(OH) are detected. Only the spectra of the sample TF0.5I, recorded in this wavenumber region, are shown in fig. 7, as for the other samples the situation is fairly close. According to these data, adsorption should follow scheme (2), as a decrease in the intensity of the band at 3725 cm^{-1}, due to free hydroxyl groups [24] is observed, with the simultaneous increase in the intensity of the broad band at 3350 cm^{-1}, probably due to ν(OH) of hydrogen bonded water molecules. In such a case, the $\delta(H_2O)$ band of molecular water would be recorded close to 1620 cm^{-1}, but it would be overlapped by the strong band due to ν_{as}(COO).

3.4. PHOTOREACTIVITY TESTS

The results are reported in fig. 8 in semilogarithmic scale as C/C_0 versus reaction time where C and C_0 are the 4-nitrophenol concentrations at time t and at time 0, respectively.

It is evident from the observation of the figure that the presence of the dopant does not influence or is detrimental on the photoreactivity. It is worth to note that a net decrease of photoreactivity occurs in the case of specimens containing iron con-

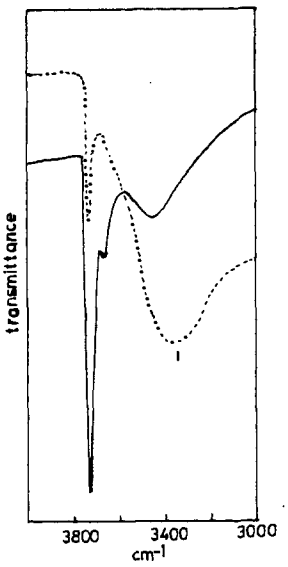

Fig. 7. FTIR spectra (ν_{OH} region) for sample TF0.5I after standard treatment (solid line) and after adsorption of methanoic acid at room temperature (dotted line).

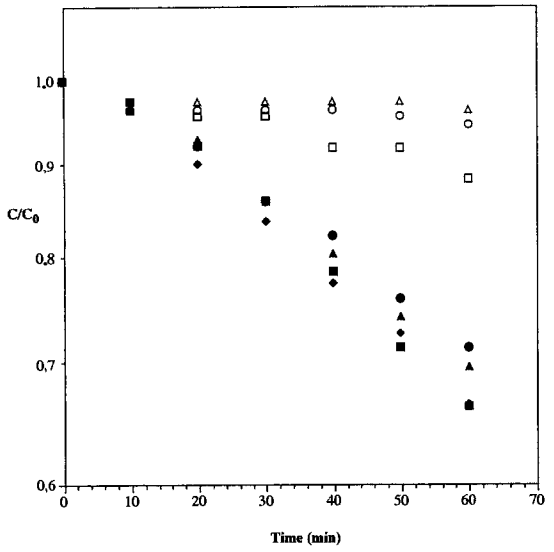

Fig. 8. 4-nitrophenol concentrations ratio, C/C_0, in semilogarithmic scale, where C and C_0 are the concentrations at time t and at time 0, versus reaction time. Catalyst concentration 1 g ℓ^{-1}; initial pH = 4.5. (■) TiO_2 "hp"; (●) TF0.02I; (▲) TF0.04I; (◆) TF0.1I; (□) TF0.5I; (○) TF1.0I; (△) TF5.0I.

centrations higher than 0.1%. For these specimens (TF0.5I; TF1.0I; TF5.0I) the photoreactivity became less and less significant as the iron content increased.

It is not the aim of this paper to deal with the mechanistic and kinetic aspects of 4-nitrophenol photodegradation, as they are reported in literature [14]. This photoreaction has been chosen only as a "test" reaction to get information about the influence of iron ions on the photoreactivity of pure titania in the above described liquid–solid system.

The preparation of TF*X*I specimens was carried out differently from that reported in literature for other similar sets of specimens [2,11]. Polycrystalline TiO_2 "hp" was impregnated instead of the amorphous solid deriving from the precipitation of Ti^{3+} species with ammonia. Moreover the temperature of heating was 823 K instead of 773 K.

This modification would have allowed one to get a more facile diffusion of iron in the lattice of titania anatase, preventing, on the other hand, anatase → rutile phase transformation, as anatase quantitatively transforms to rutile only for temperatures equal or higher to about 923 K. It is well known, indeed, that the photoreactivity of rutile phase is negligible in this regime for these kinds of photoreactions owing to kinetic constraints [25].

The presence of iron ions did not beneficially influence the photoactivity of pure TiO_2 (anatase) for the photodegradation of 4-nitrophenol, in our experimental conditions. It has been reported in literature [10] that, for other sets of specimens based on polycrystalline TiO_2 doped with chromium or iron ions, the

photoreactivity was not influenced or was detrimentally influenced in the case of photo-oxidation reactions carried out in aqueous liquid–solid regime, whereas the presence of the metal ion was essential in gas–solid regime for the photoreduction of dinitrogen to ammonia.

An explanation of the not-positive influence of the presence of iron ions as dopant of titania in the case of photo-oxidation processes occurring in aqueous liquid–solid regime can be given also for TF*X*I specimens, by taking into account the following points: (i) pure anatase–electrolyte interface exhibits the essential conditions for the occurrence of the reaction, i.e. a correct oxidation potential and an efficient charge separation, due to the formation of a Schottky barrier; (ii) the presence of iron could induce a displacement of the Fermi level; (iii) the presence of iron could influence the adsorption of the reagent species on the surface; (iv) the diffusion length of the minority carriers is strongly influenced by the presence of iron species (2 μm for iron-ion-doped TiO_2 against 1 μm for pure TiO_2) [26]; (v) the excess of iron, finally, produces on the catalyst surface layers and/or islands of inactive amorphous and/or crystalline material (Fe_2O_3, for instance).

The resulting photoactivity derives from a balance of the above factors, some of which play contrasting roles.

The characterization results indicate that the structural and the surface features, in particular the surface acid–base properties, of the doped specimens, are similar to those of pure TiO_2 "hp"; consequently the adsorption–desorption of the substrate, of the intermediates and of the products should not be significantly different. The photoreactivity, for the light doped specimens is similar to that of pure titania. For the more heavily doped specimens (iron content higher than 0.1%) the photoreactivity is negatively influenced by the presence of iron probably owing to the decrease of the density of surface active centers. The presence of Fe_2O_3 is probably not effective for O_2 reduction and for the photo-oxidation of 4-nitrophenol.

Finally, it is worth to note that a relevant influence on the photoreactivity by Fe_2O_3 detached from the surface of the photocatalyst is unlikely as (i) for the specimens having an iron content less than 3% the X-ray measurements did not indicate the presence of a separate Fe_2O_3 phase and (ii) for the specimens with a content of 5% atomic iron, the X-ray diffractograms show weak lines that can be attributed to Fe_2O_3 phase, but the photoactivity of these specimens is negligible.

Acknowledgement

The authors acknowledge to Professor G. Busca (Genoa, Italy) for his comments about the FTIR results. Some of the authors (LP, MS, AS) wish to thank Ministero dell'Università e della Ricerca Scientifica e Tecnologica (Rome) for financial support.

References

[1] R.I. Bickley, T. Gonzalez-Carreño and L. Palmisano, Mater. Chem. Phys. 29 (1991) 475.
[2] R.I. Bickley, J.S. Lees, J.D. Tilley, L. Palmisano and M. Schiavello, J. Chem. Soc. Faraday Trans. 88 (1992) 377, and references therein.
[3] J.A. Navio, M. Macias, M. Gonzalez-Catalan and A. Justo, J. Mater. Sci. 27 (1992) 3036.
[4] A.B. Rives, T.S. Kulkarni and A.L. Schwaner, Langmuir 9 (1993) 192.
[5] R.I. Bickley, T. Gonzalez-Carreño, A.R. Gonzalez-Elipé, G. Munuera and L. Palmisano, in preparation.
[6] N. Schrauzer and T.D. Guth, J. Am. Chem. Soc. 99 (1977) 7189.
[7] V. Augugliaro, A. Lauricella, L. Rizzuti, M. Schiavello and A. Sclafani, Int. J. Hydrogen Energy 7 (1982) 845.
[8] V. Augugliaro, F. D'Alba, L. Rizzuti, M. Schiavello and A. Sclafani, Int. J. Hydrogen Energy 7 (1982) 851.
[9] K. Tennakone, S. Wickramanayake, C.A.N. Fernando, O.A. Ileperuma and S. Punchihewa, J. Chem. Soc. Chem. Commun. (1987) 1078.
[10] L. Palmisano, V. Augugliaro, A. Sclafani and M. Schiavello, J. Phys. Chem. 92 (1988) 6710.
[11] J. Soria, J.C. Conesa, V. Augugliaro, L. Palmisano, M. Schiavello and A. Sclafani, J. Phys. Chem. 95 (1991) 274, and references therein.
[12] S. Lowell, *Introduction to Powder Surface Area* (Wiley, New York, 1979).
[13] V. Augugliaro, L. Palmisano, A. Sclafani, C. Minero and E. Pelizzetti, Toxicol. Environ. Chem. 16 (1988) 89.
[14] V. Augugliaro, E. Davi, L. Palmisano, M. Schiavello and A. Sclafani, Appl. Catal. 65 (1990) 101.
[15] B.C. Lippens and J.H. de Boer, J. Catal. 4 (1948) 319.
[16] L.H. Cohan, J. Am. Chem. Soc. 60 (1938) 433.
[17] H. Knözinger, Adv. Catal. 25 (1976) 184.
[18] H.A. Benesi and B.H.C. Winquist, Adv. Catal. 27 (1978) 97.
[19] C. Martin, I. Martin, V. Rives, L. Palmisano and M. Schiavello, J. Catal. 134 (1992) 434.
[20] A.M. Venezia, L. Palmisano, M. Schiavello, C. Martin, I. Martin and V. Rives, submitted.
[21] A.A. Davydov, in: *Infrared Spectroscopy of Adsorbed Species on the Surface of Metal Oxides*, ed. C.H. Rochester (Wiley, Chichester, 1990).
[22] N.W. Alcock, V.M. Tracy and T.C. Waddington, J. Chem. Soc. Dalton Trans. (1976) 2243.
[23] T.A. Stephenson, S.M. Morehouse, A.R. Powell, J.P. Heffer and G. Wilkinson, J. Chem. Soc. (1965) 3632.
[24] M. Primet, P. Pichat and M.V. Mathieu, J. Phys. Chem. 75 (1971) 1216.
[25] A. Sclafani, L. Palmisano and E. Davi, New J. Chem. 14 (1990) 265.
[26] H.P. Maruska and A.K. Ghosh, Solar Energy Mater. 1 (1979) 237.